symmetry

MDPI

Article

Settlement of an Existing Tunnel Induced by Crossing Shield Tunneling Involving Residual Jacking Force

Tianyu Liu [1], Xuehui Jiang [1], Wenjun Luo [1,*] and Jianwei Yan [1,2]

[1] Jiangxi Key Laboratory of Disaster Prevention-Mitigation and Emergency Management, East China Jiaotong University, Nanchang 330013, China; liutianyu2021@foxmail.com (T.L.); jiangxh2020@126.com (X.J.); tyanjianwei@jnu.edu.cn (J.Y.)

[2] Engineering Research & Development Centre for Underground Technology of Jiangxi Province, East China Jiaotong University, Nanchang 330013, China

* Correspondence: lwj06051979@163.com

Abstract: An analytical formulation involving residual force is proposed to predict the displacement of an existing structure by simplifying the tunnel as an infinite Euler–Bernoulli beam resting on a two-parameter Pasternak foundation. The feasibility is confirmed by two actual measurements at sites in the published literature. Parametric studies—including consideration of jacking force alone, jacking force and ground loss, and jacking force and equivalent bending stiffness—are carried out to study the influence on the deformation of the existing tunnel. The results show that the residual jacking force can decrease the settlement of the existing tunnel, but the significance of its effect varies under different engineering conditions. With the increase in ground loss, the beneficial effect of jacking force in preventing further aggravation of tunnel settlement gradually becomes obvious, and the jacking force can reduce the deformation more effectively when the tunnel has lower bending stiffness. As a result, it is recommended that some effective measures should be adopted to maintain sufficient residual jacking force in the segments, so as to prolong the life of the tunnel.

Keywords: jacking force; Euler–Bernoulli beam; Pasternak foundation; shield tunneling; tunnel deformation

Citation: Liu, T.; Jiang, X.; Luo, W.; Yan, J. Settlement of an Existing Tunnel Induced by Crossing Shield Tunneling Involving Residual Jacking Force. *Symmetry* **2022**, *14*, 1462. https://doi.org/10.3390/sym14071462

Academic Editor: Jan Awrejcewicz

Received: 7 June 2022
Accepted: 7 July 2022
Published: 18 July 2022

1. Introduction

With the speedy construction of urban rail transit in recent years in China, the utilization of underground space has encountered many challenges, such as the problem of deformation of existing tunnels induced by shield tunneling. Shield tunneling is extensively adopted as a common excavation method, which brings about the adverse consequence that the surrounding soil is inevitably disturbed, causing cracks, leakage, and other adverse impacts on adjacent existing structures [1,2]. Many scholars have conducted investigations on these adverse effects on existing tunnels [3–5]. In general, the methodologies can be classified into four categories of approaches: theoretical analysis [6–8], numerical simulation [9–12], physical model testing [13,14], and field monitoring [15–17].

There are two typical foundation models used commonly in the theoretical research field: One is the pioneer Winkler model [18], as shown in Figure 1a. Based on this model, Liu et al. [19] put forward a superposition method to research the final deflection of an existing tunnel due to new shield tunneling without clearance. In [7], the authors adopted a variation of the coefficient of subgrade reaction rather than a constant to figure out the mechanical response of the existing tunnel, and its feasibility was verified by the finite element method. However, it is noteworthy that springs in the Winkler model are independent; thus, the deformation of the foundation lacks continuity. To solve this issue, a shear layer can be added to the spring layer, resulting in a new version of the model—Pasternak foundation [20], as shown in Figure 1b. Tanahashi [21] applied the Pasternak foundation model to deduce the analytical solutions of displacements and stresses for an infinite Euler–Bernoulli beam. Liu et al. [22] employed the two-stage method to estimate the deflection of existing tunnels induced by undercrossing tunnels, and confirmed its accuracy through a comparison between finite element analysis and measured results.

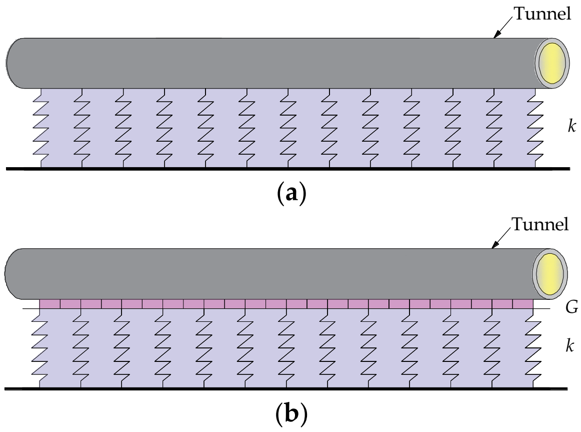

Figure 1. Two kinds of foundation models: (**a**) Winkler foundation; (**b**) Pasternak foundation.

Among the abovementioned models, the residual jacking force in the segmental lining that remains after the segment ring's installation is neglected for the sake of simplification. Nevertheless, the pressure on the segment rings does not dissipate completely even after the tunnel is in service. Li et al. [23] examined the influence of axial forces using longitudinal equivalent continuous models, and found that the increase in force yields an increase in bending stiffness. Liao et al. [24] measured the longitudinal stress relaxation up to 60% on average for shield tunnels in soft soil. Arnau et al. [25] proposed a formulation involving longitudinal creep coefficient to predict residual compressive stress along the tunnel, which was in good agreement with numerical simulations.

At present, there is a disagreement on the effect of jacking force. On the one hand, some think that the squeezing action of jacking force increases the flexural rigidity of the tunnel and, thus, profitably reduces the settlement [23,24]. On the other hand, others think that the compressive jacking force along the tunnel axis makes it much more likely to be unstable [26–28]; that is, this compressive force yields a much more severe settlement problem. Therefore, this paper aims to determine the settlement change rule versus the jacking force, and performs quantification analysis to reveal its impact. The two-stage approach is applied, and the existing tunnel is modelled as an infinite Euler–Bernoulli beam resting on a Pasternak foundation. In Step 1, the additional load produced by the ground movement is evaluated. Then, the bending deflection of the existing tunnel is explored by imposing the additional load in Step 2. The theoretical solutions are then compared with experimental measurements for verification. Parametric studies—such as jacking force, simultaneous action of the force and ground loss, and simultaneous action of the force and equivalent bending stiffness—are carried out to characterize the deformation behaviors of existing tunnels for guiding practical tunnel design.

2. Longitudinal Deformation of the Existing Tunnel

2.1. Governing Differential Equations

The calculation model of the existing tunnel under the additional load $P(x)$ is shown in Figure 2.

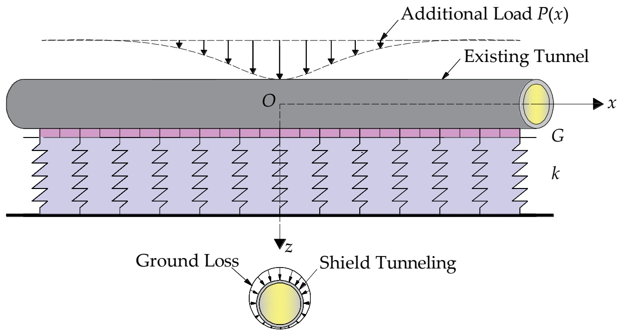

Figure 2. Calculation model.

According to Euler–Bernoulli beam theory, we have:

$$EI\frac{d^4w}{dx^4} + qD = PD \tag{1}$$

where EI and w are the equivalent bending stiffness and deformation of the existing tunnel, respectively, q is the subgrade reaction, P is the additional load, and D is the outer diameter of the existing tunnel.

Taking the longitudinal force N into account, the force equilibrium for the element is shown in Figure 3.

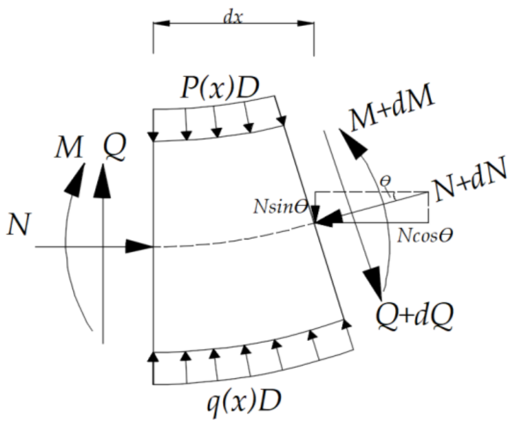

Figure 3. Beam element.

According to the plane assumption, the bending angle θ induced by the settlement can be written as follows:

$$\sin\theta = \frac{dw}{dx} \tag{2}$$

Therefore, Equation (1) can be amended as follows:

$$EI\frac{d^4w}{dx^4} - N\frac{d^2w}{dx^2} + qD = PD \tag{3}$$

The subgrade reaction q in Pasternak modal can be obtained as follows [22]:

$$q = kw - G\frac{d^2w}{dx^2} \tag{4}$$

where k is the coefficient of subgrade modulus, and G is the coefficient of shear-layer stiffness.

Combining Equations (3) and (4) yields:

$$EI\frac{d^4w}{dx^4} - (N + GD)\frac{d^2w}{dx^2} + kDw = PD \tag{5}$$

2.2. Derivation of the Solution

There are some methods employed to figure out the solutions of higher-order differential equations, such as the eigenvalue method [7,19], the finite difference procedure [29], etc. This paper adopts the finite difference approach. The existing tunnel is divided into $n + 5$ elements with length l (Figure 4), in which four extra virtual nodes need to be added at the two ends of the tunnel. Therefore, the differential equation is rewritten as follows:

$$EI\frac{w_{i+2} - 4w_{i+1} + 6w_i - 4w_{i-1} + w_{i-2}}{l^4} + kDw_i - (N + GD)\frac{w_{i+1} - 2w_i + w_{i-1}}{l^2} = DP \quad (6)$$

where w_i is the displacement at the i-th node ($i = -2, -1, \ldots, i, \ldots, n + 1, n + 2$).

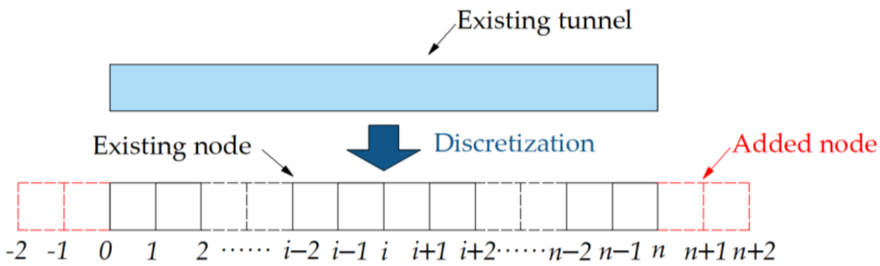

Figure 4. Diagram of tunnel discretization.

The above equation can be expressed in matrix form as follows:

$$[K]_{(n+1)\times(n+1)}[w]_{(n+1)\times 1} = [P]_{(n+1)\times 1} \quad (7)$$

where $[K]$ is the total stiffness matrix ($[K] = [K_1] + [K_2] - [K_3]$), while $[w]$ and $[P]$ are the displacement vector and the load vector along the longitudinal direction of the tunnel, respectively.

The following boundary conditions exist at both ends of the tunnel [29]:

$$\begin{cases} M_0 = EI\frac{w_1 - 2w_0 + w_{-1}}{l^2} = 0 \\ M_n = EI\frac{w_{n+1} - 2w_n + w_{n-1}}{l^2} = 0 \end{cases} \quad (8)$$

$$\begin{cases} Q_0 = EI\frac{w_2 - 2w_1 + 2w_{-1} - w_{-2}}{2l^3} = 0 \\ Q_n = EI\frac{w_{n+2} - 2w_{n+1} + 2w_{n-1} - w_{n-2}}{2l^3} = 0 \end{cases} \quad (9)$$

Combining Equations (8) and (9) will yield the solutions of w_{-2}, w_{-1}, w_{n+1}, and w_{n+2}.

At the same time, the specific content of the stiffness matrix $[K_i]$ can be determined as follows:

$$[K_1] = \frac{EI}{l^4}\begin{bmatrix} 2 & -4 & 2 & & & & & & \\ -2 & 5 & -4 & 1 & & & & & \\ 1 & -4 & 6 & -4 & 1 & & & & \\ & 1 & -4 & 6 & -4 & 1 & & & \\ & & \ddots & \ddots & \ddots & \ddots & \ddots & & \\ & & & 1 & -4 & 6 & -4 & 1 & \\ & & & & 1 & -4 & 6 & -4 & 1 \\ & & & & & 1 & -4 & 5 & -2 \\ & & & & & & 2 & -4 & 2 \end{bmatrix}_{(n+1)\times(n+1)} \quad (10)$$

$$[K_2] = kD \begin{bmatrix} 1 & & & & & & & & \\ & 1 & & & & & & & \\ & & 1 & & & & & & \\ & & & 1 & & & & & \\ & & & & \ddots & & & & \\ & & & & & 1 & & & \\ & & & & & & 1 & & \\ & & & & & & & 1 & \\ & & & & & & & & 1 \end{bmatrix}_{(n+1)\times(n+1)} \tag{11}$$

$$[K_3] = (\frac{N+GD}{l^2}) \begin{bmatrix} 0 & 0 & 0 & & & & & & \\ 1 & -2 & 1 & & & & & & \\ & 1 & -2 & 1 & & & & & \\ & & 1 & -2 & 1 & & & & \\ & & & \ddots & \ddots & \ddots & & & \\ & & & & 1 & -2 & 1 & & \\ & & & & & 1 & -2 & 1 & \\ & & & & & & 1 & -2 & 1 \\ & & & & & & 0 & 0 & 0 \end{bmatrix}_{(n+1)\times(n+1)} \tag{12}$$

Eventually, the final solution of settlement can be acquired by using the following formula:

$$[w] = [K]^{-1}[P] \tag{13}$$

2.3. Parameter Determination

In Equation (6), the parameters k, G, and P must be given. Based on Vesic's empirical formula [30], Attewell et al. [31] modified and improved the solution, for the reason that the former was obtained under an infinite beam resting on the ground surface; however, the tunnel is usually buried at a certain depth.

$$k = \frac{1.3E_s}{B(1-v^2)} \sqrt[12]{\frac{E_s B^4}{EI}} \tag{14}$$

where E_s is the elastic modulus of the soil, v is Poisson's ratio, and B is the width of the beam section (D in this paper).

Then, the influence of the embedment depth was quantified by Yu et al. [32], where the following coefficient η was proposed:

$$\eta = \begin{cases} 2.18 & z/D \leq 0.5 \\ 1 + \frac{1}{1.7z/D} & z/D > 0.5 \end{cases} \tag{15}$$

where z is the buried depth of the existing tunnel in this paper.

Thus, the calculation formula of k is updated as follows:

$$k = \frac{1.3E_s}{\eta D(1-v^2)} \sqrt[12]{\frac{ED^4}{EI}} \tag{16}$$

The coefficient of shear-layer stiffness G in the Pasternak foundation is given by Tanahashi, as follows [21]:

$$G = \frac{E_s t}{6(1+v)} \tag{17}$$

where t is the depth of the elastic layer.

According to Xu [33], the stiffness of the soil within 2.5D below the bottom of the tunnel is significantly greater than that of the shallow soil; the value of t in the process of estimating the deformation of the existing tunnel is thus taken as:

$$t = 2.5D \tag{18}$$

The schematic diagram (Figure 2) describes the deformation behavior of the existing tunnel under an additional load induced by shield tunneling. The additional load P imposed on the existing tunnel is induced by tunnel excavation. The vertical displacement $u(x, z)$ of the surrounding soil is as follows [34]:

$$\begin{aligned} u(x,z) = \; & R^2\varepsilon_0\left\{-\frac{z-H_0}{x^2+(z-H_0)^2} - \frac{2z\left[x^2-(z+H_0)^2\right]}{\left[x^2+(z+H_0)^2\right]} + (3-4v)\frac{z+H_0}{x^2+(z+H_0)^2}\right\} \\ & \exp\left\{-\left[\frac{1.38x^2}{(H_0+R)^2}+\frac{0.69z^2}{{H_0}^2}\right]\right\} \end{aligned} \tag{19}$$

where R is the radius of the new tunnel, ε_0 is the ground loss caused by excavation, and H_0 is the vertical distance between the axis of the new tunnel and the surface, as shown in Figure 5.

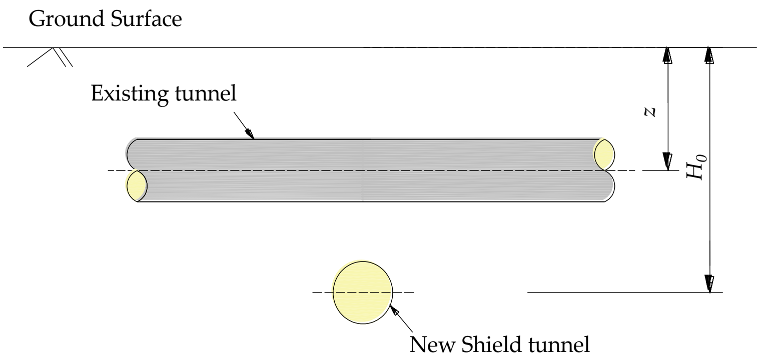

Figure 5. Relative location of the new and existing tunnels.

Therefore, the additional load P imposed on the existing tunnel can be written as follows [22]:

$$P = ku - G\frac{d^2u}{dx^2} \tag{20}$$

If there is an intersection angle β between the new tunnel and the existing tunnel, x is replaced by $x\sin\beta$ in Equation (19) [35].

3. Results and Discussions

We first verified our method by conducting two examples. Two projects of Shanghai shield tunnels crossing existing tunnels in the literature [36,37] were selected for comparison.

3.1. Case Studies

3.1.1. Case 1

Firstly, a new tunnel crossing an existing tunnel in Shanghai [36] was selected as an example. The two tunnels are designed to be almost perpendicular. The tunnel-related parameters can be seen in Table 1. The elastic modulus of the soil is 16.49 MPa, and Poisson's ratio is 0.30 [36]. According to the construction experience of the Shanghai tunnel crossing, the ground loss is taken as 0.75% [36]. The equivalent bending stiffness is 1.59×10^5 MN·m^2 [36], and the residual jack force of the existing tunnel is 60 MN [24]—the same parameters as in the next case.

Table 1. Tunnel-related parameters.

Case	Tunnel	Buried Depth (m)	Diameter (m)	Lining Thickness (m)
1	New	20.1	6.2	0.35
	Existing	9.1	6.2	0.35
2	New	25.1	6.2	0.35
	Existing	17.1	6.2	0.35

Buried depth is the distance from the ground surface to the tunnel axis, and the diameter is measured from the outside of the tunnel ring (outer diameter).

As can be observed from Figure 6, the maximum value predicted by the present theoretical solution is 7.16 mm—quite close to that of experimental measurement (about 6.0 mm); the difference 1.16 mm. Although this seems to indicate the difference is relatively large, as a matter of fact, the soil where the tunnel is buried is composed of multiple soil layers; however, these layers are usually simplified as a single isotropic soil layer in analytical study. Since the complexity of the underground soil layers and the support type in the process of building tunnels are ignored in theoretical research, it seems impossible to precisely match theoretical solutions with experimental measurements in some engineering projects. Nevertheless, the trends of the tunnel deformations calculated by the proposed method are consistent with the observed values in general, confirming the feasibility of the method.

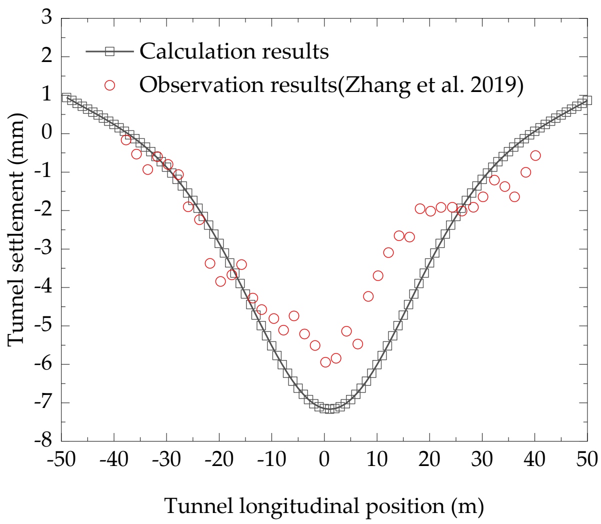

Figure 6. Comparison of observation and theoretical predictions for the existing tunnel settlement [36].

3.1.2. Case 2

Shanghai Rail Transit Line 11 undercrossing the existing Line 4 was selected as another case study [37]. The elastic modulus of the soil is 21.0 MPa, and Poisson's ratio is 0.26 [37]. The ground loss is 0.30% according to the synchronous grouting work condition. The intersection angle of the two tunnels is 75°, and more detailed soil parameters can be seen in [37].

As can be observed from Figure 7, the prediction is reasonably consistent with the on-site measurement from a global perspective. The theoretically predicted maximum settlement is 2.66 mm, while the experimental measurement is about 2.3 mm—a difference of 0.36 mm, which again confirms the feasibility of the present theoretical solution.

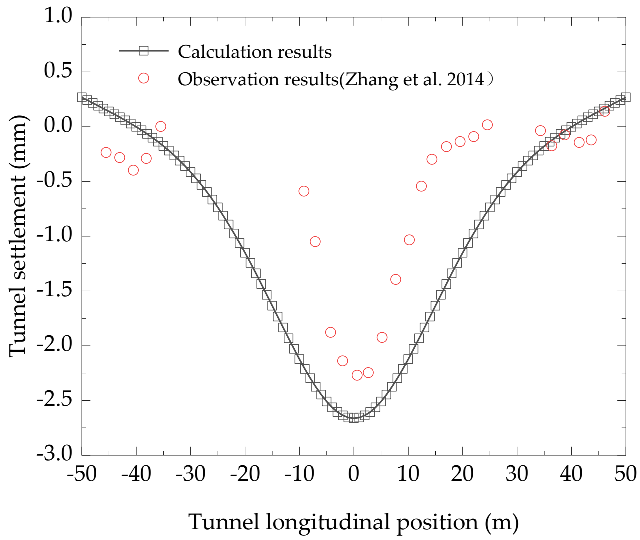

Figure 7. Comparison of observed and calculated existing tunnel settlement values [37].

3.2. Parametric Analysis

Parametric studies were carried out regarding the following three aspects: jacking force, simultaneous action of the force and ground loss, and simultaneous action of the force and equivalent bending stiffness, to analyze their influence on the bending deformation of the existing tunnel. It should be noted that all values of relevant parameters of the tunnel and soil were taken from Case 2 in Section 3.1.

3.2.1. Jacking Force

Prefabricated Grade C50–C60 reinforced concrete segments are commonly used. Thus, the maximum jacking force is no more than about 200 MN. Three values of jacking forces (0, 100, and 200 MN) were employed for analysis.

Figure 8 depicts settlement curves for the existing tunnel under different residual jacking loads. The settlement slightly decreases as the jacking force increases. The maximum settlement values are 2.68, 2.65, and 2.62 mm under jacking forces of 0, 100, and 200 MN, respectively. From the results, it seems that the residual jacking force has a slight alleviating effect on the settlement deformation of the existing tunnel. Thus, further research was carried out, as described in the following sections.

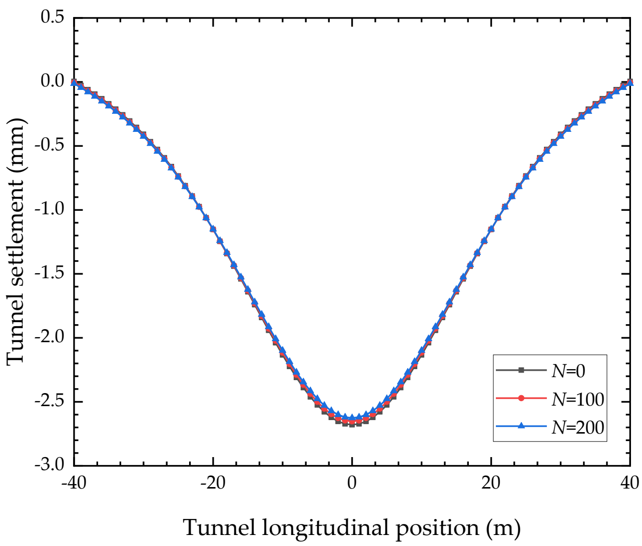

Figure 8. Analytical results with different jacking force.

3.2.2. Ground Loss and Jacking Force

Ground loss ε_0 is in the range of 0.06~2.72% in Shanghai [38]. Thus, the values of two and three times 0.75%, i.e., 1.50% and 2.25%, were selected for analysis. Two factors—ground loss and jacking force—were considered at the same time here. From Figure 9a, it can be clearly seen that the spacing of curves of analytical results under N = 0 and N = 200 MN becomes larger and larger as ground loss increases from 0.75% to 2.25%. The reductions in deformation are about 0.14 mm, 0.27 mm, and 0.40 mm, separately (Figure 9b). The beneficial effect of jacking force gradually becomes obvious as the value of ground loss increases. In tunnel structures, insufficient residual jacking force leads to displacement of the circumferential joints; furthermore, it affects the properties of the waterproofing. Therefore, it is suggested that the segments should be cured in sufficient time to maintain the residual longitudinal force, improving the service performance of the structure.

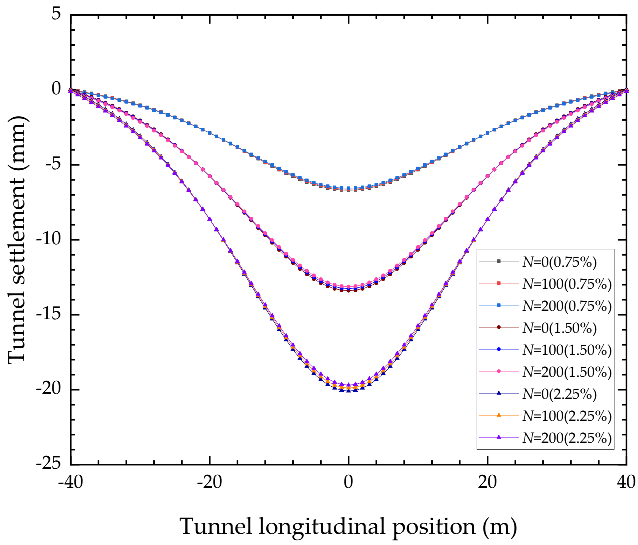

(**a**)

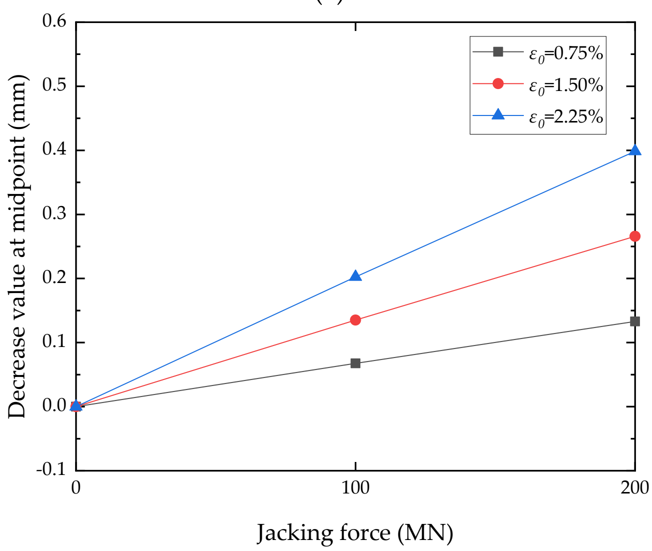

(**b**)

Figure 9. Analytical results with different jacking force and ground loss: (**a**) Results considering two factors. (**b**) Decrease in value.

3.2.3. Equivalent Bending Stiffness and Jacking Force

The various values of equivalent bending stiffness are employed in this section. Figure 10 shows the influence of jacking force on the settlement when the structure has different stiffness values. The reduction values of tunnel settlement at 0 and 200 MN, are about 0.039 mm, 0.053 mm, 0.072 mm, and 0.13 mm, respectively, under the four different values of bending stiffness. The results show that when the tunnel has a lower bending stiffness, the jacking force has a more effective settlement alleviation. In the construction process, the method of installation of the metro tunnel affects the equivalent bending stiffness of the structure [39], including non-staggered and staggered methods; the effect of the jacking force on deformation reduction thus deserves attention.

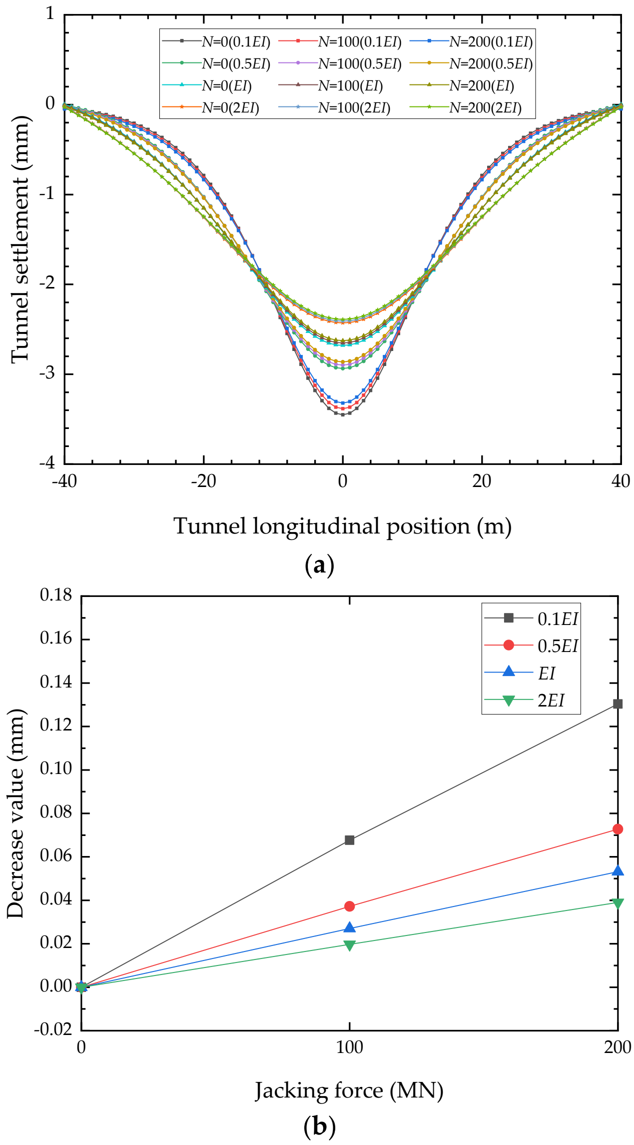

Figure 10. Analytical results with different jacking force and equivalent bending stiffness: (**a**) Results considering two factors. (**b**) Decrease in value.

4. Concluding Remarks

In this paper, an analytical solution considering residual jacking force is proposed to evaluate the settlement of an existing tunnel induced by shield crossing construction. The existing tunnel is treated as an infinite Euler–Bernoulli beam model resting on a Pasternak foundation. The two-stage approach is adopted in the theoretical research. The feasibility of this proposed method is validated by comparison with on-site measurements from previous studies. The results reveal that the theoretically predicted settlement is generally consistent with the actual measurements. Finally, parametric studies—considering jacking force, the simultaneous action of jacking force and ground loss, and the simultaneous action of jacking force and equivalent bending stiffness—are investigated to characterize the deformation of the tunnel. It follows that the jacking force can reduce the deformation, but the effect is different under different engineering conditions. When the ground loss is greater during tunnel construction, the inhibition effect of jacking force on the settlement of the existing tunnel is more obvious. In addition, the jacking force can reduce the deformation more effectively when the tunnel has lower bending stiffness. It is therefore suggested that some effective measures should be taken to maintain the residual jacking force in the segments to improve the service performance of the tunnel.

Author Contributions: Methodology, validation, writing—original draft preparation, T.L.; investigation, software, X.J.; conceptualization, project administration, W.L.; supervision, writing—review and editing, J.Y. All authors have read and agreed to the published version of the manuscript.

Funding: This research was funded by the National Natural Science Foundation of China, grant number No. 51978265, and the Jiangxi Key Laboratory of Disaster Prevention–Mitigation and Emergency Management Foundation, grant number No. 20212BCD42011.

Data Availability Statement: The authors confirm that the data supporting the findings of this study are available within the article.

Conflicts of Interest: The authors declare no conflict of interest.

References

1. Liu, D.; Zuo, J.; Wang, J.; Zhang, T.; Liu, H. Large deformation mechanism and concrete-filled steel tubular support control technology of soft rock roadway—A case study. *Eng. Fail. Anal.* **2020**, *116*, 104721. [CrossRef]
2. Zhang, J.; Zhao, M. Experimental study on mechanical behavior of the skew joints of shield tunnels under large eccentric compressive loading. *Tunn. Undergr. Space Technol.* **2021**, *111*, 103876. [CrossRef]
3. Zhou, Z.; Chen, Y.; Liu, Z.; Miao, L. Theoretical prediction model for deformations caused by construction of new tunnels undercrossing existing tunnels based on the equivalent layered method. *Comput. Geotech.* **2020**, *123*, 103565. [CrossRef]
4. Cheng, H.; Chen, R.; Wu, H.; Meng, F.; Yi, Y. General solutions for the longitudinal deformation of shield tunnels with multiple discontinuities in strata. *Tunn. Undergr. Space Technol.* **2021**, *107*, 103652. [CrossRef]
5. Zheng, G.; Pan, J.; Li, Y.; Cheng, X.; Tan, F.; Du, Y.; Li, X. Deformation and protection of existing tunnels at an oblique intersection angle to an excavation. *Int. J. Geomech.* **2020**, *20*, 05020004. [CrossRef]
6. Liang, L.; Xu, C.; Zhu, B.; Deng, J. Theoretical method for an elastic infinite beam resting on a deformable foundation with a local subsidence. *Comput. Geotech.* **2020**, *127*, 103740. [CrossRef]
7. Liu, X.; Fang, Q.; Zhang, D.; Wang, Z. Behaviour of existing tunnel due to new tunnel construction below. *Comput. Geotech.* **2019**, *110*, 71–81. [CrossRef]
8. Ke, W.; Luo, W.; Fang, T.; Chen, Q.; Xu, C.; Yan, J. A simple closed-form solution for kinematic responses of retaining wall incorporating the effects of shear stiffness of soils. *Soil Dyn. Earthq. Eng.* **2020**, *134*, 106163. [CrossRef]
9. Huang, F.; Zhang, M.; Wang, F.; Ling, T.; Yang, X. The failure mechanism of surrounding rock around an existing shield tunnel induced by an adjacent excavation. *Comput. Geotech.* **2020**, *117*, 103236. [CrossRef]
10. Chen, R.; Chen, S.; Wu, H.; Liu, Y.; Meng, F. Investigation on deformation behavior and failure mechanism of a segmental ring in shield tunnels based on elaborate numerical simulation. *Eng. Fail. Anal.* **2020**, *117*, 104960. [CrossRef]
11. Avgerinos, V.; Potts, D.M.; Standing, J.R. Numerical investigation of the effects of tunnelling on existing tunnels. *Geotechnique* **2017**, *67*, 808–822. [CrossRef]
12. Xue, F.; Zhang, M. Excavation Face Stability of Shield Tunneling Closely Under Existing Tunnels: Particle Flow Simulation. *IJST-T Civ. Eng.* **2020**, *44*, 497–506. [CrossRef]
13. Wang, H.; Liu, W.; Sun, H.; Zhuang, X. Model Test Study on the Influence of Tunnel Construction on Existing Pipeline Under the Condition of Pipeline Leakage. *Indian Geotech. J.* **2020**, *50*, 700–709. [CrossRef]
14. Ng, W.W.C.; Boonyarak, T.; David, M. Effects of Pillar Depth and Shielding on the Interaction of Crossing Multitunnels. *J. Geotech. Geoenviron.* **2015**, *141*, 04015021. [CrossRef]
15. Jin, D.; Yuan, D.; Li, X.; Zheng, H. An in-tunnel grouting protection method for excavating twin tunnels beneath an existing tunnel. *Tunn. Undergr. Space Technol.* **2018**, *71*, 27–35. [CrossRef]
16. Jin, D.; Yuan, D.; Li, X.; Zheng, H. Analysis of the settlement of an existing tunnel induced by shield tunneling underneath. *Tunn. Undergr. Space Technol.* **2018**, *81*, 209–220. [CrossRef]
17. Chen, R.; Lin, X.; Kang, X.; Zhong, Z.; Liu, Y.; Zhang, P.; Wu, H. Deformation and stresscharacteristics of existing twin tunnels induced by close-distance EPBS under-crossing. *Tunn. Undergr. Space Technol.* **2018**, *82*, 468–481. [CrossRef]
18. Winkler, E. *Die Lehre von der Elasticitaet und Festigkeit*; H. Dominicus: Prague, Czech Republic, 1867.
19. Liu, X.; Fang, Q.; Zhang, D. Mechanical responses of existing tunnel due to new tunnelling below without clearance. *Tunn. Undergr. Space Technol.* **2018**, *80*, 44–52. [CrossRef]

20. Parsternak, P.L. *On a New Method of Analysis of an Elastic Foundation by Means of Two Foundation Constants*; Gosudarstvennoe Izdatelstvo Literaturipo Stroitelstvu Arkhitekture: Moscow, Russia, 1954.
21. Tanahashi, H. Formulas for an infinitely long Bernoulli-Euler beam on the Pasternak model. *Soils Found.* **2004**, *44*, 109–118. [CrossRef]
22. Liu, Z.; Xue, J.F.; Ye, J.Z.; Qian, J. A simplified two-stage method to estimate the settlement and bending moment of upper tunnel considering the interaction of undercrossing twin tunnels. *Transp. Geotech.* **2021**, *29*, 100558. [CrossRef]
23. Li, X.; Zhou, X.; Hong, B.; Zhu, H. Experimental and analytical study on longitudinal bending behavior of shield tunnel subjected to longitudinal axial forces. *Tunn. Undergr. Space Technol.* **2019**, *86*, 128–137. [CrossRef]
24. Liao, S.; Men, Y.; Xiao, M.; Zhang, D. Field tests on longitudinal stress relaxation along shield tunnel in soft ground. *Chin. J. Geotech. Eng.* **2017**, *39*, 795–803.
25. Arnau, O.; Molins, C.; Blom, C.B.M.; Walraven, J.C. Longitudinal time-dependent response of segmental tunnel linings. *Tunn. Undergr. Space Technol.* **2012**, *28*, 98–108. [CrossRef]
26. Huang, Y.; Li, X. An analytic approach for exactly determining critical loads of buckling of nonuniform columns. *Int. J. Struct. Stab. Dyn.* **2012**, *12*, 1250027. [CrossRef]
27. Avcar, M. Elastic Buckling of Steel Columns Under Axial Compression. *Am. J. Civil. Eng.* **2014**, *2*, 102–108. [CrossRef]
28. Ings, N.L.; Trahair, N.S. Beam and column buckling under directed loading. *J. Struct. Fire Eng.* **1986**, *113*, 1251–1263. [CrossRef]
29. Liang, R.; Xia, T.; Huang, M.; Lin, C. Simplified analytical method for evaluating the effects of adjacent excavation on shield tunnel considering the shearing effect. *Comput. Geotech.* **2017**, *81*, 167–187. [CrossRef]
30. Vesic, A.B. Bending of beams resting on isotropic elastic solid. *J. Soil Mech. Found. Eng. ASCE* **1961**, *87*, 35–53.
31. Attewell, P.B.; Yeates, J.; Selby, A.R. *Soil Movement Induced by Tunnelling and Their Effects on Pipelines and Structures*; Blackie and Son Ltd.: London, UK, 1986.
32. Yu, J.; Zhang, C.; Huang, M. Soil–pipe interaction due to tunnelling: Assessment of Winkler modulus for underground pipelines. *Comput. Geotech.* **2013**, *50*, 17–28. [CrossRef]
33. Xu, L. Study on the Longitudinal Settlement of Shield Tunnel in Soft Soil. Ph.D. Thesis, Tongji University, Shanghai, China, 2005.
34. Loganathan, N.; Poulos, H.G. Analytical prediction for tunneling-induced ground movements in clays. *J. Geotech. Geoenviron.* **1998**, *124*, 846–856. [CrossRef]
35. Liang, R.; Zong, M.; Kang, C.; Wu, W.; Fang, Y.; Xia, T. Longitudinal impacts of existing shield tunnel due to down-crossing tunnelling considering shield tunnel shearing effect. *J. Zhejiang Univ. Eng. Sci.* **2018**, *52*, 20–430, 472.
36. Zhang, D.; Huang, Z.; Li, Z.; Zong, X.; Zhang, D. Analytical solution for the response of an existing tunnel to a new tunnel excavation underneath. *Comput. Geotech.* **2019**, *108*, 197–211. [CrossRef]
37. Zhang, Z.; Huang, M. Geotechnical influence on existing subway tunnels induced by multiline tunneling in Shanghai soft soil. *Comput. Geotech.* **2014**, *56*, 121–132. [CrossRef]
38. Wu, C.; Zhu, Z. Statistical analysis of ground loss ratio caused by different tunnel construction methods in China. *J. Zhejiang Univ. Eng. Sci.* **2019**, *53*, 19–30.
39. Huang, H.; Xu, L.; Yan, J.; Yu, Z. Study on transverse effective rigidity ratio of shield tunnels. *Chin. J. Geotech. Eng.* **2006**, *28*, 11–18.